

Weak radiative decays of antitriplet bottomed baryons in light-front quark model

Chao-Qiang Geng, Chia-Wei Liu, Zheng-Yi Wei , and Jiabao Zhang 

School of Fundamental Physics and Mathematical Sciences, Hangzhou Institute for Advanced Study, UCAS, Hangzhou 310024, China

 (Received 16 February 2022; accepted 6 April 2022; published 26 April 2022)

We study the weak radiative decays of $\mathbf{B}_b \rightarrow \mathbf{B}_n \gamma$ with $\mathbf{B}_{b(n)}$ the antitriplet bottomed (octet) baryons in the light-front quark model. We obtain that $\mathcal{B}(\Lambda_b \rightarrow \Lambda \gamma) = (7.1 \pm 0.3) \times 10^{-6}$, which agrees well with the current experimental value of $(7.1 \pm 1.7) \times 10^{-6}$. We predict that $\mathcal{B}(\Xi_b^0 \rightarrow \Xi^0 \gamma) = (1.0 \pm 0.1) \times 10^{-5}$ and $\mathcal{B}(\Xi_b^- \rightarrow \Xi^- \gamma) = (1.1 \pm 0.1) \times 10^{-5}$, which are consistent with the latest upper limits set by the LHCb Collaboration. In addition, we find that the $SU(3)_F$ flavor symmetry breaking effects for the modes related to the $b \rightarrow d \gamma$ transition can be as large as 20%.

DOI: [10.1103/PhysRevD.105.073007](https://doi.org/10.1103/PhysRevD.105.073007)

I. INTRODUCTION

It is known that in the weak radiative decays associated with the $b \rightarrow s \gamma$ transition the photons are purely left handed in the standard model (SM) to $\mathcal{O}(m_s^2/m_b^2)$ precision. Clearly, a signal of the right-handed photons in the experiment would be a smoking gun of new physics [1–9]. However, as the photon polarizations cannot be measured directly at the current experimental b facilities, such as LHCb, we have to analyze the cascade decays of hadrons to extract the polarization information [10–14]. In addition, since the two-body radiative decays are factorizable, the processes have a clean background for the theoretical computation.

Recently, the LHCb Collaboration has reported the following decay branching ratios [15,16]:

$$\begin{aligned} \mathcal{B}(\Lambda_b \rightarrow \Lambda \gamma) &= (7.1 \pm 1.7) \times 10^{-6}, \\ \mathcal{B}(\Xi_b^- \rightarrow \Xi^- \gamma) &< 1.3 \times 10^{-4}, \end{aligned} \quad (1)$$

which are the same sizes as the charmless nonleptonic two-body decays. Remarkably, the LHCb Collaboration has also measured the lifetimes of the antitriplet bottomed baryons (\mathbf{B}_b) with high precision [17,18] and carried out a full angular analysis for $\Lambda_b \rightarrow J/\psi \Lambda$ [19]. These results in the baryon decays clearly provide great opportunities to test the SM. On the theoretical side, the radiative bottom decays of $\mathbf{B}_b \rightarrow \mathbf{B}_n \gamma$ with \mathbf{B}_n the low-lying octet baryons have

been studied with many approaches, such as the heavy quark effective theory [20], perturbative QCD [21], $SU(3)_F$ flavor symmetry [22], light-cone sum rule (LCSR) [23,24], Bethe-Salpeter equation (BSE) [25], quark model (QM) [26–29], and effective Lagrangian [30]. In this paper, we adopt the light-front quark model (LFQM), where the quark spins and the center-of-mass motions of hadrons can be treated in a consistent and fully relativistic manner, as the wave functions of the baryons are manifestly boost invariant.

The LFQM has been extensively studied in the mesonic processes [31–43] as well as the baryon semileptonic and nonleptonic ones [44–50]. However, in the LFQM, the transition form factors can only be calculated in the nontime-like region. To obtain the form factors in the timelike region, where the semileptonic and nonleptonic decays occur, certain q^2 dependencies must be assumed, reducing the predicting power of the LFQM. In contrast, such a drawback does not exist in $\mathbf{B}_b \rightarrow \mathbf{B}_n \gamma$, allowing the LFQM to be tested more rigorously.

As a complement, we also show the results from the $SU(3)_F$ flavor symmetry similar to those in Ref. [22], which works well in the bottomed meson [51–59] and baryon decays [60–65] as well as the charmed meson [66–70] and baryon decays [65,71–79], and compare them with our evaluations from the LFQM.

This paper is organized as follows. In Sec. II, we present the formalisms for the decay widths and the tensor form factors. The numerical results and discussions are given in Sec. III. We conclude in Sec. IV.

II. FORMALISMS

We consider the weak radiative decays of antitriplet bottomed baryons induced by the quark transitions of

Published by the American Physical Society under the terms of the Creative Commons Attribution 4.0 International license. Further distribution of this work must maintain attribution to the author(s) and the published article's title, journal citation, and DOI. Funded by SCOAP³.

$b \rightarrow f\gamma$ with $f = (s, d)$. We ignore the contributions from W -exchange diagrams since they are suppressed by the CKM (Cabibbo-Kobayashi-Maskawa) elements. The effective Hamiltonians from the transitions are given by [80]

$$\mathcal{H}_{\text{eff}}(b \rightarrow f\gamma) = -\frac{G_F}{\sqrt{2}} \frac{e}{4\pi^2} V_{if}^* V_{ib} C_{7\gamma}^{\text{eff}}(\mu_b) m_b [\bar{f} i\sigma^{\mu k} (1 + \gamma^5) b] \epsilon_\mu, \quad (2)$$

where $\sigma^{\mu k} = \frac{i}{2}(\gamma^\mu \gamma^\nu - \gamma^\nu \gamma^\mu) k_\nu$, and $C_{7\gamma}^{\text{eff}}(\mu_b)$ corresponds to the effective Wilson coefficient at the scale of μ_b with $C_{7\gamma}^{\text{eff}}(5.09 \text{ GeV}) = -0.303$. The decay amplitudes are obtained by sandwiching \mathcal{H}_{eff} with the initial and final states,

$$\begin{aligned} \mathcal{M}(\mathbf{B}_b \rightarrow \mathbf{B}_n \gamma) &= -\frac{G_F}{\sqrt{2}} \frac{e}{4\pi^2} V_{if}^* V_{ib} C_{7\gamma}^{\text{eff}}(\mu_b) m_b \langle \mathbf{B}_n | \bar{f} i\sigma^{\mu k} (1 + \gamma^5) b | \mathbf{B}_b \rangle \epsilon_\mu. \end{aligned} \quad (3)$$

The matrix elements above can be parametrized in terms of the tensor form factors, given by

$$\begin{aligned} \langle \mathbf{B}_n | \bar{f} i\sigma^{\mu k} b | \mathbf{B}_b \rangle &= \bar{u}_{\mathbf{B}_n} [f_1^{TV}(k^2)(\gamma^\mu k^2 - k^\mu \not{k}) / M_{\mathbf{B}_b} \\ &\quad - f_2^{TV}(k^2) i\sigma^{\mu k}] u_{\mathbf{B}_b}, \\ \langle \mathbf{B}_n | \bar{f} i\sigma^{\mu k} \gamma^5 b | \mathbf{B}_b \rangle &= \bar{u}_{\mathbf{B}_n} [f_1^{TA}(k^2)(\gamma^\mu k^2 - k^\mu \not{k}) / M_{\mathbf{B}_b} \\ &\quad - f_2^{TA}(k^2) i\sigma^{\mu k}] \gamma^5 u_{\mathbf{B}_b}, \end{aligned} \quad (4)$$

where $u_{\mathbf{B}_{b(n)}}$ stands for the Dirac spinor of $\mathbf{B}_{b(n)}$, M the baryon mass, and k^μ the momentum transfer between the initial and final states. In our case of the radiative decays, $k^2 = 0$. We neglect the contributions associated with the form factors of $f_1^{TV}(k^2)$ and $f_1^{TA}(k^2)$ unless particularly noted in the rest of this paper. Consequently, the decay rates are given as

$$\begin{aligned} \Gamma(\mathbf{B}_b \rightarrow \mathbf{B}_n \gamma) &= \frac{\alpha_{em}}{64\pi^4} G_F^2 m_b^2 M_{\mathbf{B}_b}^3 |V_{if}^* V_{ib}|^2 (C_{7\gamma}^{\text{eff}})^2 \\ &\quad \times \left(1 - \frac{M_{\mathbf{B}_n}^2}{M_{\mathbf{B}_b}^2}\right)^3 (|f_2^{TV}|^2 + |f_2^{TA}|^2). \end{aligned} \quad (5)$$

with α_{em} the fine-structure constant of the electromagnetic interaction.

Unfortunately, to calculate the form factors of $f_2^{TV,TA}(k^2)$, the baryon wave functions are required, which cannot be reliably obtained from the first principle due to the nonperturbative effect. In this work, we use the approach in the LFQM for the baryon wave functions, in which a baryon state with momentum P and spin (S, S_z) is expressed as [31,32,49,50,81–84]

$$\begin{aligned} |B, P, S, S_z\rangle &= \sum_{\lambda_1, \lambda_2, \lambda_3} \int \{d^3 \tilde{p}_1\} \{d^3 \tilde{p}_2\} \{d^3 \tilde{p}_3\} 2(2\pi)^3 \\ &\quad \times \frac{1}{\sqrt{P^+}} \delta^3(\tilde{P} - \tilde{p}_1 - \tilde{p}_2 - \tilde{p}_3) \\ &\quad \times \Psi^{SS_z}(\tilde{p}_1, \tilde{p}_2, \tilde{p}_3, \lambda_1, \lambda_2, \lambda_3) \\ &\quad \times C^{\alpha\beta\gamma} F_{abc} |q_\alpha^a(\tilde{p}_1, \lambda_1) q_\beta^b(\tilde{p}_2, \lambda_2) q_\gamma^c(\tilde{p}_3, \lambda_3)\rangle, \end{aligned} \quad (6)$$

where Ψ represents the vertex function between the baryon and quarks, and $C^{\alpha\beta\gamma}(F_{abc})$ corresponds to the color (flavor) factor with $\alpha, \beta, \gamma(a, b, c)$ being its indices, with \tilde{p}_i the light-front three-momenta of the i th constituent quark, defined by

$$p_i = (p_i^-, p_i^+, p_i^1, p_i^2) = (p_i^-, \tilde{p}_i) = (p_i^-, p_i^+, p_{i\perp}), \quad (7)$$

with $p_i^\pm = p_i^0 \pm p_i^3$ and $p_i^- p_i^+ - p_{i\perp}^2 = m_i^2$. Here, the integration measure and delta function are given as

$$d^3 \tilde{p}_i \equiv \frac{d p_i^+ d^2 p_{i\perp}}{2(2\pi)^3}, \quad \delta^3(\tilde{p}) = \delta(p^+) \delta^2(p_\perp), \quad (8)$$

respectively, along with the normalization

$$\begin{aligned} \langle q_\alpha^a(\tilde{p}'_i, \lambda') | q_\alpha^a(\tilde{p}_i, \lambda) \rangle &= 2(2\pi)^3 \delta^3(\tilde{p}'_i - \tilde{p}_i) \delta_{\lambda'\lambda} \delta_{\alpha'a} \delta^{a'a}, \\ \langle \mathbf{B}, P', S', S'_z | \mathbf{B}, P, S, S_z \rangle &= 2(2\pi)^3 P^+ \delta^3(\tilde{P}' - \tilde{P}) \delta_{S'S_z}. \end{aligned} \quad (9)$$

The vertex function can be further decomposed as [31,32,85]

$$\Psi^{SS_z}(\tilde{p}_1, \tilde{p}_2, \tilde{p}_3, \lambda_1, \lambda_2, \lambda_3) = \Phi(\tilde{p}_1, \tilde{p}_2, \tilde{p}_3) \Xi^{SS_z}(\lambda_1, \lambda_2, \lambda_3), \quad (10)$$

in which Φ is the momentum distribution function, and Ξ^{SS_z} stands for the helicity wave function given as

$$\Xi^{SS_z}(\lambda_1, \lambda_2, \lambda_3) = \sum_{s_1, s_2, s_3} \prod_{i=1}^3 \langle \lambda_i | R_i^\dagger | s_i \rangle \left\langle \frac{1}{2} s_1, \frac{1}{2} s_2, \frac{1}{2} s_3 \middle| SS_z \right\rangle, \quad (11)$$

where R_i is the Melosh matrix, which brings the i th quark from its spin state to a helicity state, and $\langle \frac{1}{2} s_1, \frac{1}{2} s_2, \frac{1}{2} s_3 | SS_z \rangle$ is the Clebsch-Gordan coefficient, embodied in the spin wave function.

The explicit forms of Φ and R_i depend on the parametrization scheme of the internal motions of the constituent quarks. In our calculation, we choose the diquark scheme with the first two quarks being coupled to each other, while the other coupling schemes can be easily done by the permutations [49]. The kinematic variables are given as

$$\begin{aligned}\tilde{P} &= \tilde{p}_1 + \tilde{p}_2 + \tilde{p}_3, & \xi_3 &= \frac{p_1^+}{p_1^+ + p_2^+}, & \eta_3 &= 1 - \frac{p_3^+}{P^+}, \\ q_{3\perp} &= (1 - \xi_3)p_{1\perp} - \xi_3 p_{2\perp}, \\ Q_{3\perp} &= (1 - \eta_3)(p_{1\perp} + p_{2\perp}) - \eta_3 p_{3\perp}.\end{aligned}\quad (12)$$

Note that $(\xi_3, q_{3\perp})$ describe the internal motion within the diquark system, with $(\eta_3, Q_{3\perp})$ the relative motion between the diquark and the third quark [86]. The invariant masses are then given as

$$\begin{aligned}M_3^2 &= \frac{q_{3\perp}^2}{\xi_3(1 - \xi_3)} + \frac{m_1^2}{\xi_3} + \frac{m_2^2}{1 - \xi_3}, \\ M^2 &= \frac{Q_{3\perp}^2}{\eta_3(1 - \eta_3)} + \frac{M_3^2}{\eta_3} + \frac{m_3^2}{1 - \eta_3}.\end{aligned}\quad (13)$$

In this work, we adopt the Gaussian-type momentum wave function for the ground state baryon [31,49,50]. In this particular set of kinematic variables, we have that

$$\begin{aligned}\phi_3 &\equiv \Phi(\xi_3, q_{3\perp}, \eta_3, Q_{3\perp}) \\ &= \mathcal{N} \sqrt{\frac{\partial q_{3z}}{\partial \xi_3} \frac{\partial Q_{3z}}{\partial \eta_3}} \exp\left(-\frac{\vec{Q}_3^2}{2\beta_Q^2} - \frac{\vec{q}_3^2}{2\beta_{qq'}^2}\right),\end{aligned}\quad (14)$$

with $\mathcal{N} = (\beta_{qq'}\beta_Q\pi)^{-3/2}$ and

$$\begin{aligned}q_{3z} &= \frac{\xi_3 M_3}{2} - \frac{m_1^2 + q_{3\perp}^2}{2\xi_3 M_3}, & \vec{q}_3^2 &= q_{3\perp}^2 + q_{3z}^2, \\ Q_{3z} &= \frac{\eta_3 M}{2} - \frac{m_3^2 + Q_{3\perp}^2}{2\eta_3 M}, & \vec{Q}_3^2 &= Q_{3\perp}^2 + Q_{3z}^2,\end{aligned}\quad (15)$$

where $\beta_{qq'}$ and β_Q are the confinement energy scales within the diquark system and between the diquark and third quark, respectively. Note that we take the shape parameters as the internal kinematic freedoms to describe the diquark systems instead of the diquark masses. If the integration variables (\vec{q}, \vec{Q}) are used instead of $(\xi_3, q_{3\perp}, \eta_3, Q_{3\perp})$, we obtain that

$$\begin{aligned}\int d\xi_3 d\eta_3 d^2 q_{3\perp} d^2 Q_{3\perp} |\phi_3|^2 \\ = \int d^3 \vec{q}_3 d^3 \vec{Q}_3 \mathcal{N}^2 \exp\left(-\frac{\vec{Q}_3^2}{2\beta_Q^2} - \frac{\vec{q}_3^2}{2\beta_{qq'}^2}\right) = 1,\end{aligned}\quad (16)$$

where the wave functions are clearly Gaussian. On the other hand, the angular dependencies are embodied in R_i , given as

$$\begin{aligned}R_1 &= R_M(\eta_3, Q_{3\perp}, M_3, M) R_M(\xi_3, q_{3\perp}, m_1, M_3), \\ R_2 &= R_M(\eta_3, Q_{3\perp}, M_3, M) R_M(1 - \xi_3, -q_{3\perp}, m_2, M_3), \\ R_3 &= R_M(1 - \eta_3, -Q_{3\perp}, m_3, M),\end{aligned}\quad (17)$$

with

$$R_M(\xi, q_{\perp}, m, M) = \frac{m + \xi M - i\vec{\sigma} \cdot (\vec{n} \times \vec{q})}{\sqrt{(m + \xi M)^2 + q_{\perp}^2}},\quad (18)$$

where $\vec{\sigma} = (\sigma^1, \sigma^2, \sigma^3)$, representing the Pauli matrices, and $\vec{n} = (0, 0, 1)$. We emphasize that the explicit forms of R_i depend on the parametrization schemes.

As the baryon wave functions are given, we are now ready to calculate the form factors. To illustrate the calculation, we take $\Lambda_b \rightarrow \Lambda \gamma$ as an example, while the others can be obtained with slight modifications. The relevant ones in Eq. (5) can be extracted through the following equalities:

$$\begin{aligned}f_2^{TV} &= \frac{1}{4P^+} \langle \Lambda, P', \uparrow | \bar{f} i \sigma^{R+} b | \Lambda_b, P, \downarrow \rangle, \\ f_2^{TA} &= -\frac{1}{4P^+} \langle \Lambda, P', \uparrow | \bar{f} i \sigma^{R+} \gamma_5 b | \Lambda_b, P, \downarrow \rangle,\end{aligned}\quad (19)$$

where $\gamma^R = \gamma^1 + i\gamma^2$, $\gamma^+ = \gamma^0 + \gamma^3$, and the Dirac spinors in the light-front formalism can be found in the Appendix A. We choose $k^+ = 0$ to perform the calculation. In the LFQMs, this particular frame is often used to avoid the zero-mode graphs [87–91]. It has been shown that their contributions to the vector form factors vanish at the limit of $k^+ \rightarrow 0$ [31,32]. In this work, we would take it as a working assumption for the tensor ones and test it with the experimental data.

The full wave functions of Λ_b and Λ are given as

$$\begin{aligned}|\Lambda_b\rangle &= \frac{1}{\sqrt{6}} [\phi_3 \chi^{\rho^3} (|udb\rangle - |dub\rangle) + \phi_2 \chi^{\rho^2} (|ubd\rangle - |dbu\rangle) \\ &\quad + \phi_1 \chi^{\rho^1} (|bud\rangle - |bdu\rangle)], \\ |\Lambda\rangle &= \frac{1}{\sqrt{6}} [\phi_3 \chi^{\rho^3} (|uds\rangle - |dus\rangle) + \phi_2 \chi^{\rho^2} (|usd\rangle - |dsu\rangle) \\ &\quad + \phi_1 \chi^{\rho^1} (|sud\rangle - |sdu\rangle)],\end{aligned}\quad (20)$$

while the others can be found in Appendix B. In our study, since diquark clusters are viewed as effective particles, they are chosen in a way to acquire definite angular momenta. For Λ and Σ^0 , the (u, d) pairs would form the states with $J = 0$ and $J = 1$, respectively, whereas the (u, s) and (d, s) pairs would be the mixtures of $J = 0$ and $J = 1$. Thus, we choose the (u, d) pairs to form diquark clusters instead of the others. This way of constructing the baryon wave functions would break the $SU(3)$ flavor symmetry by hand, as it does not allow a diquark cluster with a light quark and a strange quark inside Λ or Σ . Such breaking effects are embedded in the expressions of the baryon octet, as the Λ and Σ baryons are taken to preserve the isospin symmetry instead of the U -spin or V -spin symmetry.

There are six terms which contribute to the transition, read as

$$\begin{aligned}
 |udb\rangle &\rightarrow |uds\rangle, & |dbu\rangle &\rightarrow |dsu\rangle, & |bud\rangle &\rightarrow |sud\rangle, \\
 |dub\rangle &\rightarrow |dus\rangle, & |ubd\rangle &\rightarrow |usd\rangle, & |bdu\rangle &\rightarrow |sdu\rangle.
 \end{aligned} \quad (21)$$

The first one in Eq. (21) contributes to the form factors as

$$\begin{aligned}
 (f_2^{TV})_{udb \rightarrow uds} &= \frac{1}{4P^+} \int d\xi_3 d\eta_3 d^2 q_{3\perp} d^2 Q_{3\perp} \phi'_3 \phi_3 F_{uds} F_{udb} \\
 &\times \sum_{\lambda'_i, \lambda_i} \Xi^{\frac{1}{2}, +\frac{1}{2}}(\lambda'_i)^\dagger \delta_{\lambda'_1 \lambda_1} \delta_{\lambda'_2 \lambda_2} (O_3^{TV})_{\lambda'_3 \lambda_3} \Xi^{\frac{1}{2}, -\frac{1}{2}}(\lambda_i),
 \end{aligned} \quad (22)$$

with

$$\begin{aligned}
 (O_3^{TV})_{\lambda'_3 \lambda_3} &= \frac{1}{1-\eta} \bar{u}(\vec{p}_3' \lambda'_3) i \sigma^{R^+} u(\vec{p}_3 \lambda_3) = -4P^+ (\sigma^R)_{\lambda'_3 \lambda_3}, \\
 (O_3^{TA})_{\lambda'_3 \lambda_3} &= \frac{1}{1-\eta} \bar{u}(\vec{p}_3' \lambda'_3) i \sigma^{R^+} \gamma_5 u(\vec{p}_3 \lambda_3) = 4P^+ (\sigma^R)_{\lambda'_3 \lambda_3},
 \end{aligned} \quad (23)$$

where $F_{uds} = F_{udb} = 1/\sqrt{6}$, and $O_3^{TV,TA}$ describes the $b \rightarrow s$ transition at the quark level, note that we have normalized σ^R as $(\sigma^1 + i\sigma^2)/2$.

On the other hand, the helicity wave functions for the initial and final baryons are

$$\begin{aligned}
 \Xi^{\frac{1}{2}, +\frac{1}{2}}(\lambda'_i)^\dagger &= \sum_{\chi_\uparrow^{\rho^3}} \prod_{i=1}^3 \langle s'_i | R'_i | \lambda'_i \rangle, \Xi^{\frac{1}{2}, -\frac{1}{2}}(\lambda_i) \\
 &= \sum_{\chi_\downarrow^{\rho^3}} \prod_{i=1}^3 \langle \lambda_i | R_i^\dagger | s_i \rangle.
 \end{aligned} \quad (24)$$

Combing them together, we get

$$\begin{aligned}
 (f_2^{TV})_{udb \rightarrow uds} &= -\frac{1}{6} \int d\xi_3 d\eta_3 d^2 q_{3\perp} d^2 Q_{3\perp} \phi'_3 \phi_3 \\
 &\times \sum_{\chi_\uparrow^{\rho^3}, \chi_\downarrow^{\rho^3}} \prod_{i=1,2} \langle s'_i | R'_i \cdot R_i^\dagger | s_i \rangle \langle s'_3 | R'_3 \cdot \sigma^R \cdot R_3^\dagger | s_3 \rangle.
 \end{aligned} \quad (25)$$

Similarly, f_2^{TA} can be obtained, given as

$$\begin{aligned}
 (f_2^{TA})_{udb \rightarrow uds} &= -\frac{1}{6} \int d\xi_3 d\eta_3 d^2 q_{3\perp} d^2 Q_{3\perp} \phi'_3 \phi_3 \\
 &\times \sum_{\chi_\uparrow^{\rho^3}, \chi_\downarrow^{\rho^3}} \prod_{i=1,2} \langle s'_i | R'_i \cdot R_i^\dagger | s_i \rangle \langle s'_3 | R'_3 \cdot \sigma^R \cdot R_3^\dagger | s_3 \rangle.
 \end{aligned} \quad (26)$$

By the permutation symmetry of the Fermi statistics, it is straightforward to see that the six transitions give exactly the same contributions to the form factors. As a result, the

transition form factors between the baryons can be obtained by multiplying Eqs. (25) and (26) by 6, given by

$$\begin{aligned}
 (f_2^{TV})_{\Lambda_b \rightarrow \Lambda} &= (f_2^{TA})_{\Lambda_b \rightarrow \Lambda} \\
 &= - \int d\xi_3 d\eta_3 d^2 q_{3\perp} d^2 Q_{3\perp} \phi'_3 \phi_3 \\
 &\times \sum_{\chi_\uparrow^{\rho^3}, \chi_\downarrow^{\rho^3}} \prod_{i=1,2} \langle s'_i | R'_i \cdot R_i^\dagger | s_i \rangle \langle s'_3 | R'_3 \cdot \sigma^R \cdot R_3^\dagger | s_3 \rangle,
 \end{aligned} \quad (27)$$

It is worth mentioning that the equality

$$f_2^{TV} = f_2^{TA} \quad (28)$$

only holds at $k^2 = 0$. This result is also consistent with that in Refs. [23,27].

The equivalence can be understood intuitively in terms of the valence quark framework, in which the spin direction of Λ is attributed to its strange quark solely. As a result, it is necessary for Λ to have the same helicity with the strange quark, which is left handed. A direct consequence is that

$$H_+ = 0, \quad (29)$$

where $H_{+(-)}$ corresponds to the helicity amplitude with the subscript denoting the helicity of Λ .

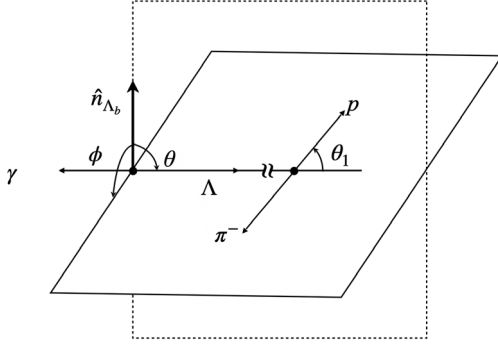
Without carrying out the numerical detail, Eq. (29) is sufficient for one to analyze the decay angular distributions. For $\Lambda_b \rightarrow \Lambda(\rightarrow p\pi^-)\gamma$, the angular dependency is given as [14,27]

$$\begin{aligned}
 \mathcal{D}(\Omega) &\equiv \frac{1}{8\pi\Gamma} \frac{1}{\partial \cos \theta \partial \cos \theta_1 \partial \phi} \frac{\partial^3 \Gamma}{\partial \cos \theta \partial \cos \theta_1 \partial \phi} \\
 &= 1 - P_b \alpha_\Lambda \cos \theta \cos \theta_1 - P_b P_L \cos \theta + \alpha_\Lambda P_L \cos \theta_1,
 \end{aligned} \quad (30)$$

where P_b is related to the Λ_b polarization and α_Λ the up-down asymmetry parameter of $\Lambda \rightarrow p\pi^-$, which can be determined by the experiments [92], and the definitions of the angles are given in Fig. 1, in which \hat{n}_{Λ_b} is the polarized direction of Λ_b . For $b \rightarrow s(d)\gamma$, the longitudinal polarization is defined by

$$P_L \equiv \frac{|H_+^2| - |H_-^2|}{|H_+^2| + |H_-^2|} = -1 + \mathcal{O}(m_{s(d)}^2/m_b^2), \quad (31)$$

where the second equality comes from Eq. (29). It is interesting to point out that the distribution is independent of ϕ due to the angular momentum conservation. Note that in contrast to $\mathbf{B}_b \rightarrow \mathbf{B}_n P$ with P a pseudoscalar meson, the up-down asymmetry parameter α_b defined through the equality of

FIG. 1. Angles in $\mathcal{D}(\vec{\Omega})$ for $\Lambda_b \rightarrow \Lambda(\rightarrow p\pi)\gamma$.

$$\frac{1}{\Gamma} \frac{\partial \Gamma}{\partial \cos \theta} \propto 1 + P_b \alpha_b \cos \theta = 1 - P_b P_L \cos \theta \quad (32)$$

has an opposite sign in respect to P_L . It is attributed to that the photon is spin-1 and transversely polarized.

III. NUMERICAL RESULTS AND DISCUSSIONS

For the CKM matrix elements, we take the Wolfenstein parametrization, given as

$$\begin{aligned} \lambda &= 0.22650 \pm 0.00048, & A &= 0.790^{+0.017}_{-0.012}, \\ \rho &= 0.141^{+0.016}_{-0.017}, & \eta &= 0.357 \pm 0.011, \end{aligned} \quad (33)$$

where the values and uncertainties are quoted from the Particle Data Group [93]. The theoretical inputs for the baryon wave functions in LFQM are given in Table I. The values of $\beta_{q_1 q'_1}$ and β_{Q_b} can be found in Ref. [50], in which β_{Q_b} are taken to be the same for all \mathbf{B}_b due to the heavy quark symmetry. The values of β_{sq_1} and β_{ss} are taken to be slightly larger than $\beta_{q_1 q'_1}$, since strange quarks are heavier than u and d , resulting in a smaller diquark system. We note that β_{sq_1} and β_{ss} are also used for β_Q of \mathbf{B}_n . Taking Ξ^0 as an example, the diquark system is made of u and s , so we have $\beta_{qq'} = \beta_{sq_1}$ and $\beta_Q = \beta_{ss}$. Our numerical results of the form factors are listed in Table II, where Ξ_b and Ξ in the second line stand for either Ξ_b^0 and Ξ^0 , or Ξ_b^- and Ξ^- , respectively.

To check our results in the LFQM, we would also like to study the decays based on the $SU(3)_F$ flavor symmetry. With $SU(3)_F$, the wave functions among the low-lying octet baryons share the identical spacial distribution, just as the wave functions of the antitriplet bottomed baryons. Consequently, by substituting $s(d)$ for b in \mathbf{B}_b and taking the inner products of the spin-flavor wave functions with \mathbf{B}_n , the relative sizes of the form factors among $\mathbf{B}_b \rightarrow \mathbf{B}_n \gamma$

TABLE I. Theoretical inputs for the baryon wave functions of the LFQM in the unit of GeV.

m_u	m_d	m_s	m_b	$\beta_{q_1 q'_1}$	β_{sq_1}	β_{ss}	β_{Q_b}
0.26	0.26	0.31	4.88	0.365	0.373	0.377	0.601

TABLE II. Form factors of $\mathbf{B}_b \rightarrow \mathbf{B}_n \gamma$.

Channel	f_2^{TV}	Channel	f_2^{TV}
$\Lambda_b \rightarrow \Lambda \gamma$	-0.123	$\Xi_b^0 \rightarrow \Sigma^0 \gamma$	-0.096
$\Xi_b^- \rightarrow \Xi^- \gamma$	0.143	$\Xi_b^- \rightarrow \Sigma^- \gamma$	-0.134
$\Lambda_b \rightarrow n \gamma$	0.135	$\Xi_b^0 \rightarrow \Lambda \gamma$	-0.056

can be determined. The $SU(3)_F$ relations [22] are given in Table III with $\lambda_{s(d)} = V_{tb} V_{ts(d)}^*$. By taking the experimental data for the branching ratio of $\Lambda_b \rightarrow \Lambda \gamma$ as a theoretical input, we can obtain the $SU(3)_F$ predictions for $\mathbf{B}_b \rightarrow \mathbf{B}_n \gamma$.

Our results of the branching ratios from the LFQM and $SU(3)_F$ are given in Table IV, where we have also shown the $SU(3)_F$ evaluations in Ref. [22] and some of other theoretical predictions in the literature, such as LCSR [23,24], BSE [25], and QM [27,29], as well as the current experimental data [15,16]. In particular, for $b \rightarrow s \gamma$ in the LFQM approach, we find that $\mathcal{B}(\Lambda_b \rightarrow \Lambda \gamma) = (7.1 \pm 0.3) \times 10^{-6}$, which agrees well with the experimental measured value. In addition, we obtain that

$$\begin{aligned} \mathcal{B}(\Xi_b^0 \rightarrow \Xi^0 \gamma) &= (1.0 \pm 0.1) \times 10^{-5}, \\ \mathcal{B}(\Xi_b^- \rightarrow \Xi^- \gamma) &= (1.1 \pm 0.1) \times 10^{-5}, \end{aligned} \quad (34)$$

which are 1.5 times larger than $\mathcal{B}(\Lambda_b \rightarrow \Lambda \gamma)$. Note that the form factors for $\Xi_b^0 \rightarrow \Xi^0 \gamma$ and $\Xi_b^- \rightarrow \Xi^- \gamma$ are exactly the same due to the isospin symmetry, but their branching ratios slightly differ due to the lifetime difference. Similarly, we have that

$$\Gamma(\Xi_b^- \rightarrow \Sigma^- \gamma) = 2\Gamma(\Xi_b^0 \rightarrow \Sigma^0 \gamma) \quad (35)$$

guaranteed by the isospin symmetry.

In addition, our LFQM results in $b \rightarrow s \gamma$ agree well with both the predictions given by $SU(3)_F$ and Refs. [23–25]. Note that the values based on $SU(3)_F$ in Ref. [22] were made within 2σ errors with respect to the experimental result of $\mathcal{B}(\Lambda_b \rightarrow \Lambda \gamma)$. Furthermore, our $SU(3)_F$ results of the center values in Table IV also slightly differ from those in Ref. [22]. These differences arise from the long-distance contributions of $\mathbf{B}_b \rightarrow \mathbf{B}_n \psi_i (\rightarrow \gamma)$ included in Ref. [22], which modify the ratios between $b \rightarrow s \gamma$ and $b \rightarrow d \gamma$.

It is interesting to see that the decay branching ratios associated with $b \rightarrow d \gamma$ in the LFQM are about 20% smaller than those predicted by the $SU(3)_F$ symmetry, which clearly show the $SU(3)_F$ breaking effects. In contrast, the ones given by Ref. [24] are larger than the

TABLE III. Amplitude ratios of $\mathbf{B}_b \rightarrow \mathbf{B}_n \gamma$ given by $SU(3)_F$.

Channel	$\Lambda_b \rightarrow \Lambda \gamma$	$\Xi_b^- \rightarrow \Xi^- \gamma$	$\Lambda_b \rightarrow n \gamma$	$\Xi_b^0 \rightarrow \Sigma^0 \gamma$	$\Xi_b^- \rightarrow \Sigma^- \gamma$	$\Xi_b^0 \rightarrow \Lambda \gamma$
Amplitude	λ_s	$-\sqrt{\frac{3}{2}}\lambda_s$	$-\sqrt{\frac{3}{2}}\lambda_d$	$\frac{\sqrt{3}}{2}\lambda_d$	$\sqrt{\frac{3}{2}}\lambda_d$	$\frac{1}{2}\lambda_d$

TABLE IV. Numerical results of the branching ratios for $\mathbf{B}_b \rightarrow \mathbf{B}_n \gamma$.

Quark level	Branching ratios	LFQM	$SU(3)_F$	$SU(3)_F$ [22]	Other models	Expt. data
$b \rightarrow s\gamma$	$10^6 \mathcal{B}(\Lambda_b \rightarrow \Lambda \gamma)$	7.1 ± 0.3	7.1 ± 1.7	7.1 ± 3.4	7.3 ± 1.5 [23] 4.0 [27] 10.0 [28]	7.1 ± 1.7 [16]
	$10^5 \mathcal{B}(\Xi_b^0 \rightarrow \Xi^0 \gamma)$	1.0 ± 0.1	1.1 ± 0.3	1.16 ± 0.60	$1.02_{-0.46}^{+0.60}$ [24]	
	$10^5 \mathcal{B}(\Xi_b^- \rightarrow \Xi^- \gamma)$	1.1 ± 0.1	1.2 ± 0.3	1.23 ± 0.64	$1.08_{-0.49}^{+0.63}$ [24]	< 13 [15]
$b \rightarrow d\gamma$	$10^7 \mathcal{B}(\Lambda_b \rightarrow n \gamma)$	4.0 ± 0.4	4.9 ± 1.2	5.03 ± 2.67	$3.69_{-1.95}^{+3.76}$ [25] 3.7 [29]	
	$10^7 \mathcal{B}(\Xi_b^0 \rightarrow \Sigma^0 \gamma)$	2.1 ± 0.2	2.6 ± 0.6	2.71 ± 1.50	$5.77_{-2.47}^{+3.16}$ [24]	
	$10^7 \mathcal{B}(\Xi_b^- \rightarrow \Sigma^- \gamma)$	4.4 ± 0.4	5.5 ± 1.3	5.74 ± 3.21	$6.14_{-2.63}^{+3.36}$ [24]	
	$10^8 \mathcal{B}(\Xi_b^0 \rightarrow \Lambda \gamma)$	7.4 ± 0.7	8.7 ± 2.1	9.17 ± 5.10		

$SU(3)_F$ predicted values. Note that the equalities of Eqs. (28) and (35) do not hold in Ref. [24]. Future experimental searches on $\Xi_b \rightarrow \Sigma \gamma$ could discriminate the various theoretical approaches.

IV. CONCLUSIONS

We have performed a systematic analysis of $\mathbf{B}_b \rightarrow \mathbf{B}_n \gamma$ based on the LFQM. We have obtained $\mathcal{B}(\Lambda_b \rightarrow \Lambda \gamma) = (7.1 \pm 0.3) \times 10^{-6}$, $\mathcal{B}(\Xi_b^0 \rightarrow \Xi^0 \gamma) = (1.0 \pm 0.1) \times 10^{-5}$, and $\mathcal{B}(\Xi_b^- \rightarrow \Xi^- \gamma) = (1.1 \pm 0.1) \times 10^{-5}$. Our results agree with the current experimental data and are consistent with other theoretical values in the literature. In addition, for $b \rightarrow s\gamma$, we have found that our results in the LFQM are in good agreement with those based on the $SU(3)_F$ symmetry. Moreover, we have demonstrated that the $SU(3)_F$ breaking effects for $b \rightarrow d\gamma$ are as large as 20%. We have also explicitly shown that $f_2^{TV} = f_2^{TA}$ at $k^2 = 0$ in the LFQM, resulting in that $P_L = -\alpha = -1 + \mathcal{O}(m_{s(d)}^2/m_b^2)$ for $b \rightarrow s(d)\gamma$, which are independent of the theoretical input. A dedicated experimental measurement of the angular distribution of $\Lambda_b \rightarrow \Lambda(\rightarrow p\pi^-)\gamma$ is strongly recommended for testing the SM and probing possible effects from new physics.

ACKNOWLEDGMENTS

We want to thank Dr. Tien-Hsueh Tsai for his valuable assistance on the numerical part of this work.

APPENDIX A: DIRAC SPINOR IN LIGHT-FRONT FORMALISM

We adopt the notation given in Ref. [32] for the light-front formalism. The Dirac spinors turn out to be

$$\begin{aligned}
 u(p, \lambda) &= \frac{1}{\sqrt{p^+}} (p^+ + \beta + \boldsymbol{\alpha}_\perp \mathbf{p}_\perp) \times \begin{cases} \chi(\uparrow) & \text{for } \lambda = +1 \\ \chi(\downarrow) & \text{for } \lambda = -1 \end{cases}, \\
 v(p, \lambda) &= \frac{1}{\sqrt{p^+}} (p^+ - \beta m + \boldsymbol{\alpha}_\perp \mathbf{p}_\perp) \times \begin{cases} \chi(\downarrow) & \text{for } \lambda = +1 \\ \chi(\uparrow) & \text{for } \lambda = -1 \end{cases},
 \end{aligned} \tag{A1}$$

where $\beta = \gamma^0$ and $\boldsymbol{\alpha}_\perp = (\gamma^0 \gamma^1, \gamma^0 \gamma^2)$ with γ^α ($\alpha = 0, 1, 2, 3$) being the Dirac gamma matrices, while the two χ spinors are given by

$$\chi(\uparrow) = \frac{1}{\sqrt{2}} \begin{pmatrix} 1 \\ 0 \\ 1 \\ 0 \end{pmatrix} \quad \text{and} \quad \chi(\downarrow) = \frac{1}{\sqrt{2}} \begin{pmatrix} 0 \\ 1 \\ 0 \\ -1 \end{pmatrix}, \tag{A2}$$

resulting in the helicity eigenstates,

$$\begin{aligned}
 u(p, +) &= \frac{1}{\sqrt{2p^+}} \begin{pmatrix} p^+ + m \\ p^1 + ip^2 \\ p^+ - m \\ p^1 + ip^2 \end{pmatrix} \quad \text{and} \\
 u(p, -) &= \frac{1}{\sqrt{2p^+}} \begin{pmatrix} -p^1 + ip^2 \\ p^+ + m \\ p^1 - ip^2 \\ -p^+ + m \end{pmatrix}.
 \end{aligned} \tag{A3}$$

Accordingly, the relations in Eq. (19) and (23) can be verified directly.

APPENDIX B: MOMENTUM-SPIN-FLAVOR WAVE FUNCTION

The momentum-spin-flavor wave functions for \mathbf{B}_b and \mathbf{B}_n are given as

$$\begin{aligned} |\Xi_b^- \rangle &= \frac{1}{\sqrt{6}} [\phi_3 \chi^{\rho 3} (|dsb\rangle - |sdb\rangle) + \phi_2 \chi^{\rho 2} (|dbs\rangle - |sbd\rangle) + \phi_1 \chi^{\rho 1} (|bds\rangle - |bsd\rangle)], \\ |\Xi_b^0 \rangle &= \frac{1}{\sqrt{6}} [\phi_3 \chi^{\rho 3} (|usb\rangle - |sub\rangle) + \phi_2 \chi^{\rho 2} (|ubs\rangle - |sbu\rangle) + \phi_1 \chi^{\rho 1} (|bus\rangle - |bsu\rangle)], \\ |\Lambda_b^0 \rangle &= \frac{1}{\sqrt{6}} [\phi_3 \chi^{\rho 3} (|udb\rangle - |dub\rangle) + \phi_2 \chi^{\rho 2} (|ubd\rangle - |dbu\rangle) + \phi_1 \chi^{\rho 1} (|bud\rangle - |bdu\rangle)], \end{aligned} \quad (\text{B1})$$

$$\begin{aligned} |p\rangle &= \frac{1}{\sqrt{3}} \phi [\chi^{\lambda 3} |uud\rangle + \chi^{\lambda 2} |udu\rangle + \chi^{\lambda 1} |duu\rangle], \\ |n\rangle &= \frac{1}{\sqrt{3}} \phi [\chi^{\lambda 3} |ddu\rangle + \chi^{\lambda 2} |dud\rangle + \chi^{\lambda 1} |udd\rangle], \\ |\Xi^0 \rangle &= \frac{1}{\sqrt{3}} [\phi_3 \chi^{\lambda 3} |ssu\rangle + \phi_2 \chi^{\lambda 2} |sus\rangle + \phi_1 \chi^{\lambda 1} |uss\rangle], \\ |\Xi^- \rangle &= \frac{1}{\sqrt{3}} [\phi_3 \chi^{\lambda 3} |ssd\rangle + \phi_2 \chi^{\lambda 2} |sds\rangle + \phi_1 \chi^{\lambda 1} |dss\rangle], \\ |\Sigma^+ \rangle &= \frac{1}{\sqrt{3}} [\phi_3 \chi^{\lambda 3} |uus\rangle + \phi_2 \chi^{\lambda 2} |usu\rangle + \phi_1 \chi^{\lambda 1} |suu\rangle], \\ |\Sigma^- \rangle &= \frac{1}{\sqrt{3}} [\phi_3 \chi^{\lambda 3} |dds\rangle + \phi_2 \chi^{\lambda 2} |dsd\rangle + \phi_1 \chi^{\lambda 1} |sdd\rangle], \end{aligned} \quad (\text{B2})$$

$$\begin{aligned} |\Sigma^0 \rangle &= \frac{1}{\sqrt{6}} [\phi_3 \chi^{\lambda 3} (|uds\rangle + |dus\rangle) + \phi_2 \chi^{\lambda 2} (|usd\rangle + |dsu\rangle) + \phi_1 \chi^{\lambda 1} (|sud\rangle + |sdu\rangle)], \\ |\Lambda \rangle &= \frac{1}{\sqrt{6}} [\phi_3 \chi^{\rho 3} (|uds\rangle - |dus\rangle) + \phi_2 \chi^{\rho 2} (|usd\rangle - |dsu\rangle) + \phi_1 \chi^{\rho 1} (|sud\rangle - |sdu\rangle)]. \end{aligned} \quad (\text{B3})$$

Here, the spin wave functions are defined as

$$\begin{aligned} \chi_{\uparrow}^{\rho 3} &= \frac{1}{\sqrt{2}} (|\uparrow \uparrow \downarrow \uparrow\rangle - |\downarrow \uparrow \uparrow \uparrow\rangle), & \chi_{\uparrow}^{\lambda 3} &= \frac{1}{\sqrt{6}} (2|\uparrow \uparrow \downarrow \downarrow\rangle - |\uparrow \downarrow \uparrow \uparrow\rangle - |\downarrow \uparrow \uparrow \uparrow\rangle), \\ \chi_{\uparrow}^{\rho 2} &= \frac{1}{\sqrt{2}} (|\uparrow \uparrow \downarrow \downarrow\rangle - |\downarrow \uparrow \uparrow \uparrow\rangle), & \chi_{\uparrow}^{\lambda 2} &= \frac{1}{\sqrt{6}} (2|\uparrow \downarrow \downarrow \uparrow\rangle - |\uparrow \uparrow \downarrow \downarrow\rangle - |\downarrow \uparrow \uparrow \uparrow\rangle), \\ \chi_{\uparrow}^{\rho 1} &= \frac{1}{\sqrt{2}} (|\uparrow \uparrow \downarrow \downarrow\rangle - |\uparrow \downarrow \uparrow \uparrow\rangle), & \chi_{\uparrow}^{\lambda 1} &= \frac{1}{\sqrt{6}} (2|\downarrow \uparrow \uparrow \uparrow\rangle - |\uparrow \downarrow \uparrow \uparrow\rangle - |\uparrow \uparrow \downarrow \downarrow\rangle). \end{aligned} \quad (\text{B4})$$

The definitions of momentum wave functions $\phi_{1,2}$ are given as

$$\phi_{1,2} \equiv \Phi(\xi_{1,2}, q_{1,2\perp}, \eta_{1,2}, Q_{1,2\perp}) = \mathcal{N} \sqrt{\frac{\partial q_{1,2z}}{\partial \xi_{1,2}} \frac{\partial Q_{1,2z}}{\partial \eta_{1,2}}} \exp\left(-\frac{\vec{Q}_{1,2}^2}{2\beta_Q^2} - \frac{\vec{q}_{1,2}^2}{2\beta_{q'}^2}\right), \quad (\text{B5})$$

$$\begin{aligned} q_{1,2z} &= \frac{\xi_{1,2} M_{1,2}}{2} - \frac{m_{2,3}^2 + q_{1,2\perp}^2}{2\xi_{1,2} M_{1,2}}, & \vec{q}_{1,2}^2 &= q_{1,2\perp}^2 + q_{1,2z}^2, \\ Q_{1,2z} &= \frac{\eta_{1,2} M}{2} - \frac{m_{1,2}^2 + Q_{1,2\perp}^2}{2\eta_{1,2} M}, & \vec{Q}_{1,2}^2 &= Q_{1,2\perp}^2 + Q_{1,2z}^2. \end{aligned} \quad (\text{B6})$$

- [1] J. C. Pati and A. Salam, *Phys. Rev. D* **10**, 275 (1974); **11**, 703(E) (1975).
- [2] R. N. Mohapatra and J. C. Pati, *Phys. Rev. D* **11**, 2558 (1975).
- [3] R. N. Mohapatra and J. C. Pati, *Phys. Rev. D* **11**, 566 (1975).
- [4] G. Senjanovic and R. N. Mohapatra, *Phys. Rev. D* **12**, 1502 (1975).
- [5] G. Senjanovic, *Nucl. Phys.* **B153**, 334 (1979).
- [6] R. N. Mohapatra and G. Senjanovic, *Phys. Rev. D* **23**, 165 (1981).
- [7] C. S. Lim and T. Inami, *Prog. Theor. Phys.* **67**, 1569 (1982).
- [8] L. L. Everett, G. L. Kane, S. Rigolin, L. T. Wang, and T. T. Wang, *J. High Energy Phys.* **01** (2002) 022.
- [9] D. Atwood, M. Gronau, and A. Soni, *Phys. Rev. Lett.* **79**, 185 (1997).
- [10] R. Aaij *et al.* (LHCb Collaboration), *J. High Energy Phys.* **12** (2020) 081.
- [11] R. Aaij *et al.* (LHCb Collaboration), *Phys. Rev. Lett.* **112**, 161801 (2014).
- [12] C. Q. Geng and C. W. Liu, *J. High Energy Phys.* **11** (2021) 104.
- [13] C. W. Liu and C. Q. Geng, *J. High Energy Phys.* **01** (2022) 128.
- [14] L. M. García Martín, B. Jashal, F. M. Vidal, A. Oyanguren, S. Roy, R. Sain, and R. Sinha, *Eur. Phys. J. C* **79**, 634 (2019).
- [15] R. Aaij *et al.* (LHCb Collaboration), *J. High Energy Phys.* **01** (2022) 069.
- [16] R. Aaij *et al.* (LHCb Collaboration), *Phys. Rev. Lett.* **123**, 031801 (2019).
- [17] R. Aaij *et al.* (LHCb Collaboration), *Phys. Rev. Lett.* **113**, 032001 (2014).
- [18] R. Aaij *et al.* (LHCb Collaboration), *Phys. Rev. Lett.* **113**, 242002 (2014).
- [19] R. Aaij *et al.* (LHCb Collaboration), *J. High Energy Phys.* **06** (2020) 110.
- [20] P. Singer and D. X. Zhang, *Phys. Lett. B* **383**, 351 (1996).
- [21] X. G. He, T. Li, X. Q. Li, and Y. M. Wang, *Phys. Rev. D* **74**, 034026 (2006).
- [22] R. M. Wang, X. D. Cheng, Y. Y. Fan, J. L. Zhang, and Y. G. Xu, *J. Phys. G* **48**, 085001 (2021).
- [23] Y. M. Wang, Y. Li, and C. D. Lu, *Eur. Phys. J. C* **59**, 861 (2009).
- [24] A. R. Olamaei and K. Azizi, *Eur. Phys. J. C* **82**, 68 (2022).
- [25] L. L. Liu, C. Wang, X. W. Kang, and X. H. Guo, *Eur. Phys. J. C* **80**, 193 (2020).
- [26] P. K. Chatley and A. C. Sharma, *Phys. Rev. D* **25**, 2351 (1982).
- [27] T. Gutsche, M. A. Ivanov, J. G. Korner, V. E. Lyubovitskij, and P. Santorelli, *Phys. Rev. D* **87**, 074031 (2013).
- [28] R. N. Faustov and V. O. Galkin, *Phys. Rev. D* **96**, 053006 (2017).
- [29] R. N. Faustov and V. O. Galkin, *Mod. Phys. Lett. A* **32**, 1750125 (2017).
- [30] H. Y. Cheng, C. Y. Cheung, G. L. Lin, Y. C. Lin, T. M. Yan, and H. L. Yu, *Phys. Rev. D* **51**, 1199 (1995).
- [31] F. Schlumpf, *Phys. Rev. D* **47**, 4114 (1993); **49**, 6246(E) (1994).
- [32] W. M. Zhang, *Chin. J. Phys.* **32**, 717 (1994), arXiv:hep-ph/9412244.
- [33] C. Q. Geng, C. C. Lih, and W. M. Zhang, *Phys. Rev. D* **57**, 5697 (1998).
- [34] C. C. Lih, C. Q. Geng, and W. M. Zhang, *Phys. Rev. D* **59**, 114002 (1999).
- [35] C. Q. Geng, C. C. Lih, and W.-M. Zhang, *Phys. Rev. D* **62**, 074017 (2000).
- [36] C. Q. Geng, C. W. Hwang, C. C. Lih, and W. M. Zhang, *Phys. Rev. D* **64**, 114024 (2001).
- [37] C. Q. Geng and C. C. Liu, *J. Phys. G* **29**, 1103 (2003).
- [38] H. Y. Cheng, C. K. Chua, and C. W. Hwang, *Phys. Rev. D* **69**, 074025 (2004).
- [39] C. Q. Geng, C. C. Lih, and C. Xia, *Eur. Phys. J. C* **76**, 313 (2016).
- [40] H. Y. Cheng and X. W. Kang, *Eur. Phys. J. C* **77**, 587 (2017); **77**, 863(E) (2017).
- [41] Q. Chang, L. T. Wang, and X. N. Li, *J. High Energy Phys.* **12** (2019) 102.
- [42] Y. J. Shi, W. Wang, and Z. X. Zhao, *Eur. Phys. J. C* **76**, 555 (2016).
- [43] Y. L. Shen and G. Li, *Eur. Phys. J. C* **73**, 2441 (2013).
- [44] Z. X. Zhao, *Eur. Phys. J. C* **78**, 756 (2018).
- [45] Z. X. Zhao, *Chin. Phys. C* **42**, 093101 (2018).
- [46] Z. P. Xing and Z. X. Zhao, *Phys. Rev. D* **98**, 056002 (2018).
- [47] C. K. Chua, *Phys. Rev. D* **99**, 014023 (2019).
- [48] C. K. Chua, *Phys. Rev. D* **100**, 034025 (2019).
- [49] C. Q. Geng, C. C. Lih, C. W. Liu, and T. H. Tsai, *Phys. Rev. D* **101**, 094017 (2020).
- [50] C. Q. Geng, C. W. Liu, and T. H. Tsai, *Phys. Lett. B* **815**, 136125 (2021).
- [51] X. G. He, *Eur. Phys. J. C* **9**, 443 (1999).
- [52] X. G. He, Y. K. Hsiao, J. Q. Shi, Y. L. Wu, and Y. F. Zhou, *Phys. Rev. D* **64**, 034002 (2001).
- [53] H. K. Fu, X. G. He, and Y. K. Hsiao, *Phys. Rev. D* **69**, 074002 (2004).
- [54] Y. K. Hsiao, C. F. Chang, and X. G. He, *Phys. Rev. D* **93**, 114002 (2016).
- [55] M. Gronau, O. F. Hernandez, D. London, and J. L. Rosner, *Phys. Rev. D* **50**, 4529 (1994).
- [56] M. Gronau, O. F. Hernandez, D. London, and J. L. Rosner, *Phys. Rev. D* **52**, 6356 (1995).
- [57] S. H. Zhou, Q. A. Zhang, W. R. Lyu, and C. D. Lu, *Eur. Phys. J. C* **77**, 125 (2017).
- [58] H. Y. Cheng, C. W. Chiang, and A. L. Kuo, *Phys. Rev. D* **91**, 014011 (2015).
- [59] N. G. Deshpande and X. G. He, *Phys. Rev. Lett.* **75**, 1703 (1995).
- [60] A. Dery, M. Ghosh, Y. Grossman, and S. Schacht, *J. High Energy Phys.* **03** (2020) 165.
- [61] X. G. He and G. N. Li, *Phys. Lett. B* **750**, 82 (2015).
- [62] M. He, X. G. He, and G. N. Li, *Phys. Rev. D* **92**, 036010 (2015).
- [63] S. Shivashankara, W. Wu, and A. Datta, *Phys. Rev. D* **91**, 115003 (2015).
- [64] P. Singer, *Nucl. Phys. B, Proc. Suppl.* **50**, 202 (1996).
- [65] W. Wang, Z. P. Xing, and J. Xu, *Eur. Phys. J. C* **77**, 800 (2017).
- [66] Y. Grossman and D. J. Robinson, *J. High Energy Phys.* **04** (2013) 067.
- [67] D. Pirtskhalava and P. Uttayarat, *Phys. Lett. B* **712**, 81 (2012).

- [68] H. Y. Cheng and C. W. Chiang, *Phys. Rev. D* **86**, 014014 (2012).
- [69] M. J. Savage, *Phys. Lett. B* **257**, 414 (1991).
- [70] S. Muller, U. Nierste, and S. Schacht, *Phys. Rev. D* **92**, 014004 (2015).
- [71] M. J. Savage and R. P. Springer, *Phys. Rev. D* **42**, 1527 (1990).
- [72] G. Altarelli, N. Cabibbo, and L. Maiani, *Phys. Lett. B* **57**, 277 (1975).
- [73] C. D. Lu, W. Wang, and F. S. Yu, *Phys. Rev. D* **93**, 056008 (2016).
- [74] C. Q. Geng, Y. K. Hsiao, Y. H. Lin, and L. L. Liu, *Phys. Lett. B* **776**, 265 (2018).
- [75] C. Q. Geng, Y. K. Hsiao, C. W. Liu, and T. H. Tsai, *Phys. Rev. D* **97**, 073006 (2018).
- [76] C. Q. Geng, Y. K. Hsiao, C. W. Liu, and T. H. Tsai, *J. High Energy Phys.* **11** (2017) 147.
- [77] C. Q. Geng, C. W. Liu, T. H. Tsai, and S. W. Yeh, *Phys. Lett. B* **792**, 214 (2019).
- [78] D. Wang, *Eur. Phys. J. C* **79**, 429 (2019).
- [79] D. Wang, P. F. Guo, W. H. Long, and F. S. Yu, *J. High Energy Phys.* **03** (2018) 066.
- [80] G. Buchalla, A. J. Buras, and M. E. Lautenbacher, *Rev. Mod. Phys.* **68**, 1125 (1996).
- [81] H. Y. Cheng, C. K. Chua, and C. W. Hwang, *Phys. Rev. D* **70**, 034007 (2004).
- [82] H. W. Ke, N. Hao, and X. Q. Li, *Eur. Phys. J. C* **79**, 540 (2019).
- [83] H. W. Ke, X. Q. Li, and Z. T. Wei, *Phys. Rev. D* **77**, 014020 (2008).
- [84] H. W. Ke, X. H. Yuan, X. Q. Li, Z. T. Wei, and Y. X. Zhang, *Phys. Rev. D* **86**, 114005 (2012).
- [85] C. Q. Geng, C. C. Lih, and W. M. Zhang, *Phys. Rev. D* **57**, 5697 (1998).
- [86] B. L. G. Bakker, L. A. Kondratyuk, and M. V. Terentev, *Nucl. Phys.* **B158**, 497 (1979).
- [87] H. M. Choi and C. R. Ji, *Phys. Rev. D* **58**, 071901 (1998).
- [88] H. M. Choi and C. R. Ji, *Phys. Rev. D* **72**, 013004 (2005).
- [89] H. M. Choi and C. R. Ji, *Phys. Lett. B* **696**, 518 (2011).
- [90] H. M. Choi and C. R. Ji, *Few Body Syst.* **52**, 409 (2012).
- [91] H. M. Choi and C. R. Ji, *Few Body Syst.* **55**, 435 (2014).
- [92] M. Ablikim *et al.* (BESIII Collaboration), *Nat. Phys.* **15**, 631 (2019).
- [93] P. Zyla *et al.* (Particle Data Group), *Prog. Theor. Exp. Phys.* **2020**, 083C01 (2020).